Response to referee #2:

We highly appreciate the referee's valuable comments and instructive suggestions. We have addressed each comment as below and corresponding revisions have been made in the manuscript.

This paper report results of vertical profiles of black carbon aerosol collected in the North China Plain. The topic and the reported measurements are very important as vertical profile data of BC a globally scarce if compared with the high amount of ground-based observation. Thus the topic of this paper is of fundamental importance. It is suitable to be published on ACP after the authors raised the following points.

MAIN POINTS: Abstract (page 1 lines 12-20): the development of the mixing layer is qualitatively described. Moreover it is reported that the mixing layer usually developed from 0.2 km up to 1 km (i.e. sunny days) and followed by a "collapse" during the evening. In a such situation a residual layer usually forms above the NBL making the concentration measured above the mixing layer not representative of a clean free troposphere. Please discuss also the possible importance of the residual layer formation on your measurements along the entire manuscript.

We thank the referee for the valuable suggestion. We agree with the referee that the existence of a residual layer would make measured BC mass concentrations (m_{BC}) above the mixing layer not representative of a clean free troposphere. As stated in the manuscript, average m_{BC} in free troposphere could reach 2~3 μg m^{-3} under polluted conditions, otherwise usually well below 1 μg m^{-3} under clean conditions. The case study of vertical profiles measured on July 1 (Fig. 6) showed a polluted layer with a thickness of 0.3 km in the morning, possibly a residual layer formed the day before. The level of m_{BC} above the polluted layer was also as high as ~2 μg m^{-3}. The case study of vertical profiles measured on July 8 (also in Fig. 6) showed how vertical profiles of m_{BC} evolved with the development of the planetary boundary layer (PBL). A relatively high level of m_{BC} was found above the NBL where the remnant of the daytime mixing layer after its collapse might be traced. However, analysis regarding the impact of the residual layer formed in the previous evening on measurements on the next day is difficult to carry out without continuous measurements from the previous day. Also the characteristics of the residual layer should be affected by the advection. The role of the residual layer in affecting the evolution of the PBL still stays controversial, though it has been consented that BC could heat the PBL and intensify atmospheric stability. Ding et al. (2016) demonstrated the importance of the "dome effect" of BC in the PBL especially the upper PBL, suppressing the PBL height and enhancing haze pollution within a lower PBL. However, Zhang et al. (2012) indicated a limited warming effect of BC in an elevated aerosol layer, and also limited induced increase in the strength of atmospheric inversion.

Corresponding discussions in the revised manuscript include:

P10, L8, "This might imply the existence of a polluted residual layer above the stable surface layer formed after the sunset in previous evening, yet unable to be further discussed without continuous measurements from the day before. Also the characteristics of m_{BC} in FT should be affected by the advection."

P10, L17, "Sometimes, a residual layer with a relatively high level of m_{BC} (>2 μg m^{-3}) could be formed above the NBL where the remnant of the daytime mixing layer might be traced after its collapse (e.g., profiles on July 8). This would undoubtedly have an impact on measured m_{BC} above the mixing layer on the next day, leading to a polluted background in FT (e.g., in the morning of July 1 and 8). The role of the residual layer in affecting the evolution of the PBL still stays controversial, though it has been consented that BC could heat the PBL and intensify atmospheric stability. Ding et al. (2016) demonstrated the importance of the "dome effect" of BC in the PBL especially the upper PBL, suppressing the PBL height and enhancing haze pollution within a lower PBL. Whereas in Zhang et al. (2012), a limited warming effect of BC in an elevated aerosol layer and limited induced increase in the strength of atmospheric inversion were indicated."

Section 2.2.1: the developed smoothing algorithm appears very promising. However, a deeper discussion here is called for. Especially it is necessary to compare the smoothing results with that can be obtained by the ONA (Hagler et al. (2011)) application. I strongly suggest to introduce a new picture to show the effect

of the two data treatment on the raw collected BC data along vertical profiles. The reason for a such request comes from the fact that the Hagler at al. algorithm is based on the physical behavior of the measured ATN in the Aethalometer, while the new smoothing algorithm reported in this paper appear only statistically based and somehow affected by the operator (i.e. "(6) Repeat step (1)-(5) for m times to obtain acceptable smoothed data"). Concerning the last point in brackets: have you defined a criteria for the "acceptable smoothed data"? How much is the threshold? How much is the loss in terms of vertical resolution of the data after the smoothing? I think the smoothing algorithm should be also discussed more quantitatively than did until now.

We agree with the referee that a comparison between processed data using the two smoothing algorithms, Fluctuation Minimizing Smoothing (FMS) method proposed in this study and the ONA method in Hagler et al. (2011), should be made to show the similarity and differences in effects of the two approaches on unsmoothed data. As found in the two cases displayed in Fig. R1 (also as Fig. 3 in the revised manuscript), generally, both algorithms properly treated data fluctuation and largely improved the presented data. However, the FMS procedure seemed to be more capable of reliably reducing data fluctuation without losing details on the variability of vertical profiles (Fig. R1d-R1f).

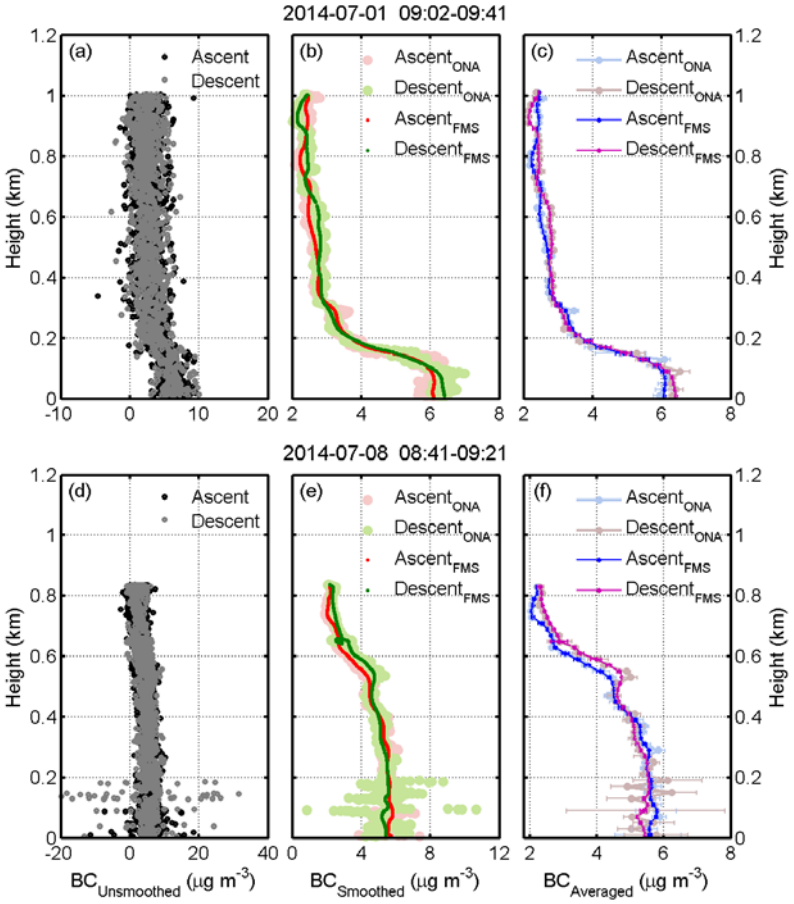

Figure R1. (a) Unsmoothed BC mass concentrations measured with a temporal resolution of 1 s on July 1, 2014 (09:02-09:41 LT). Data points collected from the ascending and descending process are respectively marked in black and grey dots. (b) Smoothed BC mass concentrations using two algorithms. Data points processed by the ONA method are displayed in large pink dots for the ascent and in light green color for the descent. Data points processed by the FMS method are denoted by small red dots for the ascent and green dots for the descent. (c) 20-m averaged profiles based upon smoothed data using two algorithms. Dots indicate 20-m averages, with standard deviations in error bars. Results from the ONA and FMS methods are respectively given in the color of light blue and blue for the ascent, while in the color of light purple and purple for the descent. (d)-(f) Measured and processed BC vertical profiles on July 8, 2014 (08:41-09:21 LT). The caption is the same as that in (a)-(c).

The FMS method was devised to smooth the highly temporally resolved data (1 s) from AE-51. Similar to the ONA method (Hagler et al., 2011), the FMS approach is also principally based upon the physical behavior of measured ATN. Usually, ATN is supposed to increase with time. However, reported ATN might largely fluctuate due to limited sampling on the filter and instrumental noises such as that from the light source, the detector, electronics, the flow rate and unstable posture. Despite that BC values determined from fluctuated ATN might drastically vary, large positive/negative BC pairs would always be found and counterbalance each other within a few seconds. Therefore, the FMS method minimizes data fluctuation by finding pairs of BC values that differ largely with each other within a few seconds and making a compromise of them. The smoothing window *n* used to search for pairs and the smoothing count used to repeat the smoothing were empirically chosen. Normally, data fluctuation is already compensated within 5 s, according to what has been observed in data processing.

To address the loss of the vertical resolution of processed data using the FMS method, the contribution from neighboring data points to the weighted average of each target point was calculated. In the FMS procedure, each data point was averaged within a range of 2*n* data points, where *n* is the smoothing window. The average process was repeated by *m* times, where *m* is the smoothing count. With *n* to be 5 and *m* to be 1 or 5, average weight function for each profile was calculated and the result was similar among profiles. When *m* was set to be 1, the average of the target point was mostly contributed from neighboring data points within about 11 seconds, according to a weight of 80%. This consequently led to a vertical resolution of about 22 m for the ascent and 11 m for the descent after smoothing. Similarly, the vertical resolution was about 50~60 m for the ascent and 25~30 m for the descent when *m* was set to be 5. Figure R2 presents average weight function for two cases as given in Fig. R1. Different choices of the smoothing count gave a similar pattern of vertical profiles, but with some differences in details. To achieve a better smoothing for further calculations, the smoothing count was chosen to be 5 in this work.

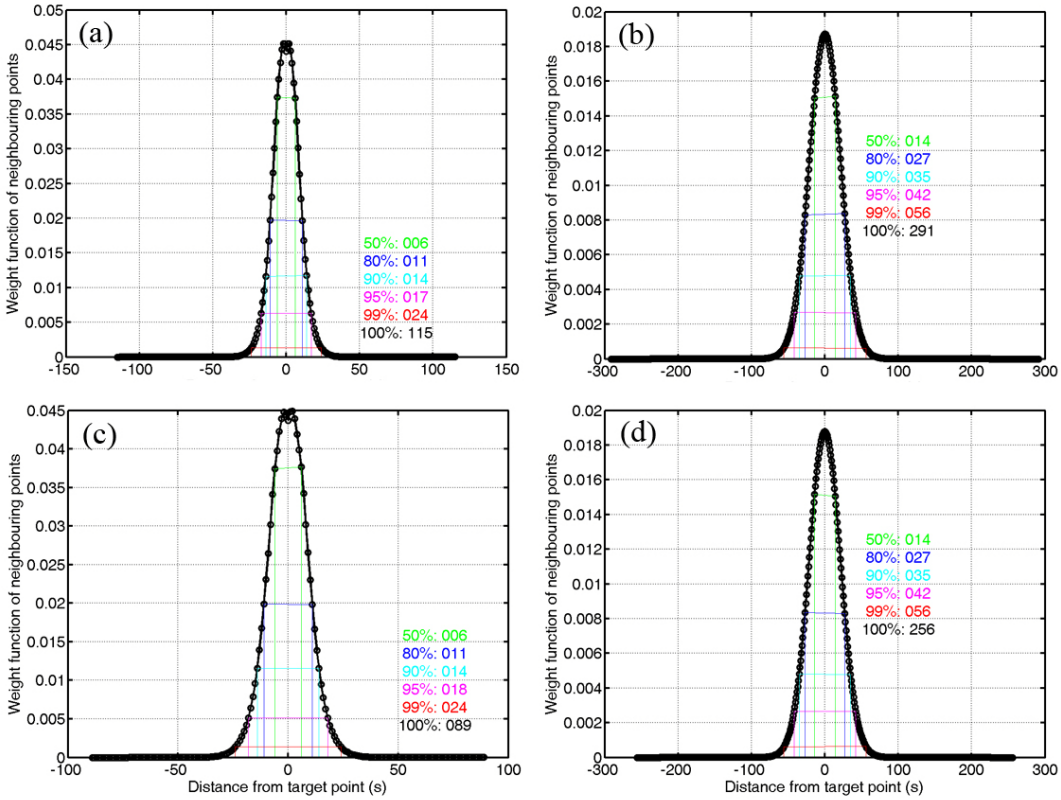

Figure R2 Average weight function of neighboring data points to show their contribution to the weighted average of each target point for the case on July 1, 2014 (09:02-09:41 LT) with the smoothing window *n* to be 5, (a) the smoothing count *m* was set to be 1; (b) *m* was set to be 5. Similar to the first case, average weight function for the case on July 8, 2014 (08:41-09:21 LT), (c) the smoothing count *m* was set to be 1; (d) *m* was set to be 5.

According to above discussions, we have revised the manuscript as:

P4, L30, "In this study, data dispersion due to high temporal resolution was treated by a new smoothing algorithm, Fluctuation Minimizing Smoothing (FMS). Similar to the ONA method, the FMS approach is also principally based upon the physical behavior of measured ATN. Despite that BC values determined from fluctuated ATN might drastically vary, large positive/negative pairs of BC values would always be found and counterbalance each other within a few seconds. Therefore, the FMS approach was devised to find pairs of BC values that differ largely with each other within a few seconds and make a compromise."

P5, L15, "The smoothing window *n* and the smoothing count *m* were empirically chosen during the calculation. It should be kept in mind that using improper large *n* or *m* might wipe off some natural variations, although it will always give a smoother result. *n* should be set to no more than 5, given that data fluctuation is normally already compensated within 5 s. With *n* to be 5 and *m* to be 1, the average of the target point was mostly contributed from neighboring data points within about 11 seconds, according to a weight of 80%. This consequently led to a vertical resolution of about 22 m for the ascent and 11 m for the descent after smoothing. Similarly, the vertical resolution was about 50~60 m for the ascent and 25~30 m for the descent when *m* was set to be 5. Different choices of *m* gave a similar pattern of vertical profiles, but with some differences in details. In this study, *m* was set to be 5 to achieve a better smoothing for further calculations, though this caused a loss of the vertical resolution more than twice as large as that when just smoothing once. A comparison was made between unsmoothed data, smoothed data using the FMS approach in this study and the ONA method in Hagler et al. (2011), as well as 20-m averaged data using those two algorithms. It was found that both algorithms could properly deal with data fluctuation caused by instrumental noises without introducing artificial features (e.g., Fig. 3a-3c). However, the FMS method seemed to be more capable of reliably removing outliers in some cases (e.g., Fig. 3d-3f). The comparison indicated that the FMS procedure could effectively reduce data fluctuation while still preserve reasonable variability of the profile."

Moreover, we have corrected a mistake in the description of the smoothing algorithm.

P5, L8, "…, where i=1,2,…,N-1,N and j=1,2,…,n-1,n;"

Section 2.2.2, page 5, line 8: "Details of the correction scheme developed for tackling with artifacts of AE-31 were described in Ran et al. (2016)". Note that Ran et al. (2016) is just a submitted paper. In the reference list the journal to which Ran et al. paper was submitted is missing. Please add it. Moreover, as the AE31 data could significantly change in function of the chosen correction function it is necessary to resume here at least the main points of the correction scheme adopted in Ran et al. as the paper is not yet available to the scientific community. With respect to this, depending on the chosen correction scheme (i.e. C factors for each wavelength of the AE31), the obtained angstrom exponent should change introducing an error on the retrieved $\sigma_{MAAP,880nm}$. A quantitative assessment of the variability of $\sigma_{MAAP,880nm}$ depending on the chosen correction scheme for the AE31 is called for. Moreover, I strongly recommend an analysis of the error propagation of $\sigma_{MAAP,880nm}$ on the obtained C for the AE51. As a matter of fact the C factor of 2.52 is reported here without any statistical treatment of its uncertainty. Finally, no reference was made to the C value of 2.05±0.03 for the AE51 reported in Ferrero et al. (2011a). It should very interesting to discuss the difference on the two C values in terms of the chemical composition of the aerosol in the NCP with respect to the Europe.

We thank the referee for the helpful and instructive comments. We agree with the referee that more details should be given on the correction scheme adopted in Ran et al. (2016), which has just been published in Atmospheric Environment.

Briefly, the correction scheme used to deal with instrumental artifacts of AE-31 was a combination of the

modified Virkkula method (Virkkula et al., 2007) to treat the shadowing effect and the Schmid method (Schmid et al., 2006) to treat filter multiple scattering and aerosol scattering effects. The modified Virkkula method assumed a linear relationship between BC mass concentrations and time across the filter change, particularly, a quadratic relationship for special cases where ambient BC experienced a peak-shaped variation, instead of the assumption of constant BC mass concentrations in Virkkula et al. (2007). Following procedures in the Schmid method, the wavelength-dependent correction factor (C_λ) could be derived. As the referee stated, the choice of the correction scheme for AE-31 measurements might introduce uncertainties to absorption Angström exponent (α), and thereby pass them to $\sigma_{MAAP,880nm}$ that were calculated from α and absorption coefficients measured at 637 nm ($\sigma_{MAAP,637nm}$) by MAAP. Using a constant C factor for AE-31 as also often used in some studies (e.g., Weingartner et al., 2003; Sandradewi et al., 2008) instead of the wavelength-dependent C_λ results in an underestimation of α over the 660-880 nm spectrum by about 19.5%. This consequently leads to an overestimation of $\sigma_{MAAP,880nm}$ and the C factor for AE-51 by about 9.6% and 8.4%, respectively.

Another important thing to mention is that the actual wavelength of MAAP is 637 nm instead of the nominal wavelength of 670 nm (Müller et al., 2011), as pointed out by one of the referees for Ran et al. (2016). We have accordingly corrected all related results in the revised manuscript. Subsequently, attenuation coefficients $\sigma_{AE\text{-}51,880nm}$ (ATN<10) measured by AE-51 and calculated $\sigma_{MAAP,880nm}$ were employed to yield the C factor using reduced major axis regression (Fig. R3, also as Fig. 2 in the revised manuscript). The C factor was 2.98±0.05 with 95% confidence, quite different from a value of 2.05±0.03 in Ferrero et al. (2011a). Possible explanations on such a difference in the C factor might be found in aerosol chemical compositions in the NCP region and the Po Valley basin. Besides, the C factor in Ferrero et al. (2011a) was obtained from Mie calculations, and thus was subject to uncertainties resulting from assumptions such as BC size distributions, BC mixing state and particle morphology. Also the C factor derived from methods in this study bears some uncertainties as mentioned above.

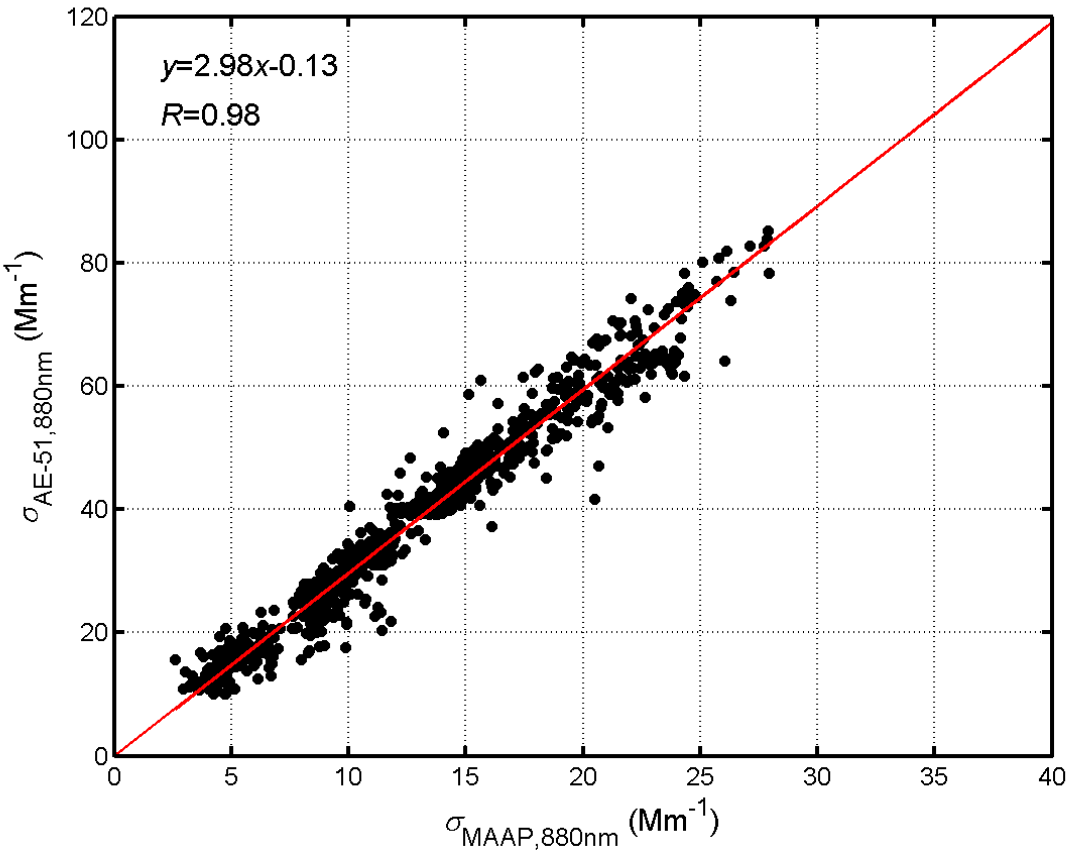

Figure R3. Reduced major axis regression of attenuation coefficients $\sigma_{AE\text{-}51,880nm}$ (ATN<10) measured by AE-51 and absorption coefficients $\sigma_{MAAP,880nm}$ calculated from concomitant MAAP and AE-31 measurements in the comparative test.

Accordingly, revisions have been made in the manuscript as:

P6, L11, "AE-31 suffered instrumental artifacts in the same way as AE-51. Details of the correction scheme developed for tackling with AE-31 artifacts were described in Ran et al. (2016). Briefly, the correction scheme combined the modified Virkkula method (Virkkula et al., 2007) to treat the shadowing effect and the Schmid method (Schmid et al., 2006) to treat filter multiple scattering and aerosol scattering effects. The modified Virkkula method assumed a linear relationship of BC mass concentrations and time across the filter change, particularly, a quadratic relationship for special cases where ambient BC experienced a peak-shaped variation, instead of constant BC mass concentrations as in Virkkula et al. (2007). The wavelength-dependent correction factor (C_λ) could be obtained following procedures in Schmid et al. (2006). The temporal resolution of AE-31 during the comparative test was 2 min."

P6, L30, "Three steps were taken to obtain the *C* factor. Firstly, aerosol absorption Angström exponent (α) over the spectrum span of 660 and 880 nm was derived from absorption coefficients $\sigma_{\text{AE-31,660nm}}$ and $\sigma_{\text{AE-31,880nm}}$, which were corrected from attenuation coefficients at 660 and 880 nm measured by AE-31. Hence, α was calculated from:

$$\alpha = \frac{\ln(\sigma_{\text{AE-31,660nm}}) - \ln(\sigma_{\text{AE-31,880nm}})}{\ln(880) - \ln(660)}. \quad (2)$$

Secondly, α for the spectrum of 660 and 880 nm was used to represent α over the span of 637 and 880 nm. Therefore, $\sigma_{\text{MAAP,880nm}}$ was quantified from measured $\sigma_{\text{MAAP,637nm}}$ following the spectral dependence of aerosol absorption coefficients in the form of $\lambda^{-\alpha}$:

$$\sigma_{\text{MAAP,880nm}} = \sigma_{\text{MAAP,637nm}} \times \left(\frac{880}{637}\right)^{-\alpha} , \quad (3)$$

Finally, reduced major axis regression of attenuation coefficients $\sigma_{\text{AE-51,880nm}}$ (ATN<10) measured by AE-51 and absorption coefficients $\sigma_{\text{MAAP,880nm}}$ calculated from MAAP and AE-31 yielded the *C* factor of 2.98±0.05 with 95% confidence (Fig. 2). It was noted that the *C* factor for AE-51 was reported as 2.05±0.03 with 95% confidence in Ferrero et al. (2011a). Possible explanations on such a difference in the *C* factor might be found in aerosol chemical compositions in the NCP region and the Po Valley basin. Besides, the *C* factor in Ferrero et al. (2011a) was obtained from Mie calculations, and thus was subject to uncertainties resulting from assumptions such as BC size distributions, BC mixing state and particle morphology. In addition, the choice of the correction scheme for AE-31 measurements in this study might introduce uncertainties to α and thereby $\sigma_{\text{MAAP,880nm}}$. Using a constant *C* factor for AE-31 as also often used in some studies (e.g., Weingartner et al., 2003; Sandradewi et al., 2008) instead of the wavelength-dependent C_λ results in an underestimation of α over the 660-880 nm spectrum by about 19.5%. This consequently leads to an overestimation of $\sigma_{\text{MAAP,880nm}}$ and the *C* factor for AE-51 by about 9.6% and 8.4%, respectively."

Page 5, lines 12-13: "Measured $\sigma_{\text{AE-51,880nm}}$ (ATN<10) and calculated $\sigma_{\text{MAAP,880nm}}$ were linearly fitted with a correlation coefficient of 0.96 in a significant level (P<0.001), yielding a C value of 2.52": Please add the picture of this correlation.

We have added a figure as Fig. 2 in the revised manuscript to show this correlation. The figure is given in the response to the last comment.

Page 6, line 13, equation 6: "H_{m} was calculated from a sigmoid function that could well characterize typical daytime profile of m_{BC}:". From this sentence it appears that H_{m} was calculated using equation 6. However, equation 6 requires as input both the mixing layer and the entrainment layer. This point is not clearly defined and needs to be specified. I also suggest to add a graphical example of the mixing layer determination using the sigmoid function. Finally a question: as you have both the potential temperature and wind profiles at disposal, have you ever thought to analyse the mixing layer also using the Richardson

number approach?

We thank the referee for pointing out the interpretation that might have caused confusion. We have added an illustration to show the fitting of BC profiles using the sigmoid function (Fig. R4, also as Fig. S4 in the supplement). We have clarified this point in the revised manuscript as:

P8, L24, "On the other hand, typical daytime profiles of m_{BC} could be well characterized by the sigmoid function:

$$m_{BC} = C_{ms} - \frac{C_{ms} - C_{fs}}{e^{-(h - H_{m,BC,sigmoid})/H_e} + 1} \quad (6)$$

where C_{ms} and C_{fs} are respectively characteristic m_{BC} within the ML and in free troposphere (FT), $H_{m,BC,sigmoid}$ is the mixing height derived from BC vertical profiles using the sigmoid function, H_e represents the thickness of the EL, h is the height at which each 20-m averaged m_{BC} is obtained. The parameters C_{ms}, C_{fs}, $H_{m,BC,sigmoid}$ and H_e could be directly determined by fitting measured m_{BC} at each height h using Eq. (6) as shown by the example (Fig. S4). A comparison was made between $H_{m,BC,gradient}$ and $H_{m,BC,sigmoid}$ for typical daytime BC vertical profiles. Results from the two methods agreed quite well with each other, with a difference of less than 2 % (Fig. S5). In addition to reliably estimating the mixing height as the gradient method, the sigmoid function could also directly determine parameters including C_{ms}, C_{fs}, and H_e. Therefore, the sigmoid function was chosen to obtain all parameters for typical daytime BC profiles."

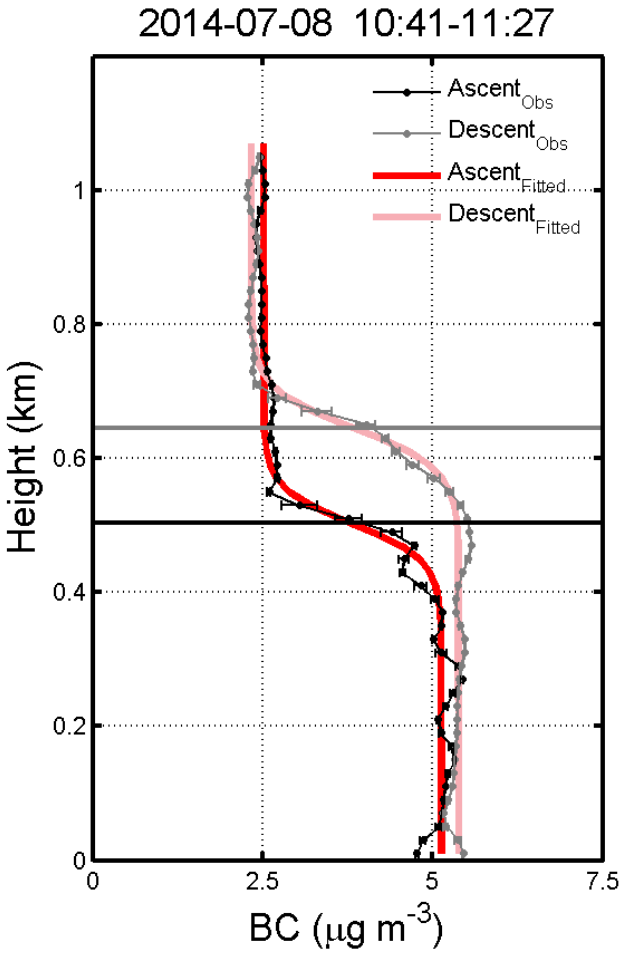

Figure R4. An example of fitting BC vertical profiles using the sigmoid function. Measurements were conducted on July 8, 2014 (10:41-11:27 LT).

Finally, we followed the referee's suggestion and employed the Richardson number approach to determine the mixing height (Vogelezang and Holtslag, 1996; Seibert et al., 2000). Equation (R1) was used to calculate the Richardson number $Ri_b(h)$ for each 5-m layer at the midpoint h, where $\theta_v(h)$ is the virtual potential temperature calculated from potential temperature and the mixing ratio of water vapor, θ_{v1} is the average virtual potential

temperature for the 5-10 m layer, $U(h)$ and $V(h)$ are wind components computed from wind speed and direction, g is the gravity of earth. The mixing height was determined as the height where $Ri_b(h)$ exceeded the classic critical value of 0.25 (Seibert et al., 2000).

$$Ri_b(h) = \frac{gh}{\theta_{v1}} \frac{\theta_{v1}(h) - \theta_{v1}}{U(h)^2 + V(h)^2} \quad \text{(R1)}$$

Figure R5 shows a satisfactory agreement among mixing heights estimated from vertical profiles of θ ($H_{m,\theta}$) and q ($H_{m,q}$) using the gradient method and from the Richardson number approach ($H_{m,RN}$). However, uncertainties in the determination of mixing heights using the Richardson number approach might arise from the accuracy of temperature and wind profiles, the choice of the equation and the critical value. Moreover, the height of the nocturnal boundary layer was poorly determined and corresponding results have been removed in Fig. R5. Therefore, a combination of the sigmoid approach and the gradient method was applied to estimate mixing heights for the entire dataset.

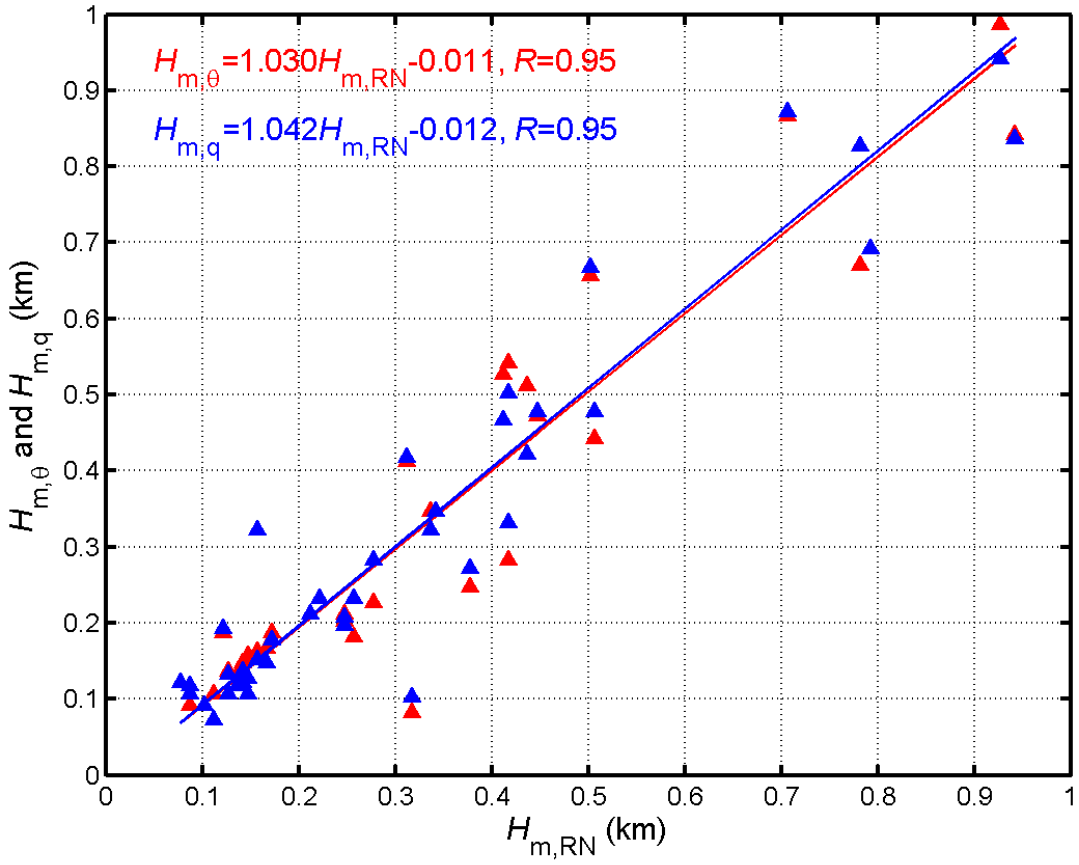

Figure R5. A comparison among mixing heights estimated from vertical profiles of θ ($H_{m,\theta}$) and q ($H_{m,q}$) using the gradient method, and that from the Richardson number approach ($H_{m,RN}$).

MINOR POINTS: Page 7, lines 3-4: "the normalized height (H_{Nor}), which was calculated from h/H_m-1". In Ferrero et al. (2014) this analysis is explained. Add this reference at the end of the sentence.

We thank the referee for this helpful comment. We have revised the manuscript as:

P9, L17, "Statistically, vertical profiles of BC were categorized into two types, according to their shapes along the normalized height (H_{Nor}), which was calculated from h/H_m-1 (Ferrero et al., 2014)."

Figure 2b: at H_{Nor}=0 BC data are characterized by free troposphere concentration levels. I was a bit surprised about it. I expected that around H_{Nor}=0 there was at least the end of the exponential decrease of concentration starting from ground values. Could you comment it?

We thank the referee for pointing this out. As expected, the height around H_{Nor}=0 is indeed the end of the exponential decrease of m_{BC} starting from the ground value for individual profile. Figure 2b (as Fig. 5b in the revised manuscript) displays each vertical profile of m_{BC} in the evening (grey lines). Above the NBL (H_{Nor}>0), no apparent decrease in m_{BC} was found for individual profile. However, the level of m_{BC} above H_{Nor}=0 differed largely in different cases, representing clean or relatively polluted conditions in FT. Hence, the average profile presents an artificial feature of a decrease in m_{BC} even above H_{Nor}=0. To clarify the confusing feature of the average profile, we have revised the manuscript as:

P9, L27, "For each BC profile (grey lines in Fig. 5b), m_{BC} nearly exponentially declined with H_{Nor}, as a result of weakened turbulence and vertical dispersion."

Page 3, lines 24-25 and equation 1: "to estimate aerosol absorption coefficients at the wavelength of 880 nm following"… Please note that $\sigma_{AE\text{-}51,880nm}$ is the attenuation coefficient and not the absorption coefficient as reported in many papers (i.e. starting from Weingartner et al. (2003)). Please correct the paper for this point.

We thank the referee for this valuable comment. We have corrected the manuscript as:

P4, L18, "…simultaneously detected to obtain attenuation coefficients at the wavelength of 880 nm ($\sigma_{AE\text{-}51,880nm}$)…"

References

Ding, A. J., Huang, X., Nie, W., Sun, N. J., Kerminen, V. M., Petäjä, T., Su, H., Cheng, Y. F., Yang, X. Q., Wang, M. H., Chi, X. G., Wang, J. P., Virkkula, A., Guo, W. D., Yuan, J., Wang, S. Y., Zhang, R. J. Zhang, Wu, Y. F., Song, Y. Song, Zhu, T., Zilitinkevich, S., Kulmala, M., and Fu, C. B.: Enhanced haze pollution by black carbon in megacities in China, Geophys. Res. Lett., 43, 2873-2879, doi:10.1002/2016GL067745, 2016.

Ferrero, L., Mocnik, G., Ferrini, B. S., Perrone, M. G., Sangiorgi, G., and Bolzacchini, E.: Vertical profiles of aerosol absorption coefficient from micro-aethalometer data and Mie calculation over Milan, Sci. Total Environ., 40, 2824-2837, doi:10.1016/j.scitotenv.2011.04.022, 2011a.

Ferrero, L., Castelli, M., Ferrini, B. S., Moscatelli, M., Perrone, M. G., Sangiorgi, G., D'Angelo, L., Rovelli, G., Moroni, B., Scardazza, F., Mocnik, G., Bolzacchini, E., Petitta, M., and Cappelletti, D.: Impact of black carbon aerosol over Italian basin valleys: high-resolution measurements along vertical profiles, radiative forcing and heating rate, Atmos. Chem. Phys., 14, 9641-9664, doi:10.5194/acp-14-9641-2014, 2014.

Hagler, G. S. W., Yelverton, T. L. B., Vedantham, R., Hansen, A. D. A. and Turner, J. R.: Post-Processing Method to Reduce Noise while Preserving High Time Resolution in Aethalometer Real-Time Black Carbon Data, Aerosol Air Qual. Res., 11, 539-546, doi:10.4209/aaqr.2011.05.0055, 2011.

Müller, T., Henzing, J. S., de Leeuw, G., Wiedensohler, A., Alastuey, A., Angelov, H., Bizjak, M., Collaud Coen, M., Engström, J. E., Gruening, C., Hillamo, R., Hoffer, A., Imre, K., Ivanow, P., Jennings, G, Sun, J. Y., Kalivitis, N., Karlsson, H., Komppula, M., Laj, P., Li, S. M., Lunder, C., Marinoni, A., Martins dos Santos, S., Moerman, M., Nowak, A., Ogren, J. A., Petzold, A., Pichon, J. M., Rodriquez, S., Sharma, S., Sheridan, P. J., Teinilä, K., Tuch, T., Viana, M., Virkkula, A., Weingartner, E., Wilhelm, R., and Wang, Y. Q.: Characterization and intercomparison of aerosol absorption photometers: result of two intercomparison workshops, Atmos. Meas. Tech., 4, 245-268, doi:10.5194/amt-4-245-2011, 2011.

Ran, L., Deng, Z. Z., Wang, P. C., and Xia, X. A.: Black carbon and wavelength-dependent aerosol absorption in the North China Plain based on two-year aethalometer measurements, Atmos. Environ., 142, 132-144, doi:10.1016/j.atmosenv.2016.07.014, 2016.

Sandradewi, J., Prevot, A. S. H., Weingartner, E., Schmidhauser, R., Gysel, M., and Baltensperger, U.: A study of wood burning and traffic aerosols in an Alpine valley using a multi-wavelength aethalometer, Atmos. Environ., 42, 101-112, doi:10.1016/j.atmosenv.2007.09.034, 2008 .

Schmid, O., Artaxo, P., Arnott, W. P., Chand, D., Gatti, L.V., Frank, G. P., Hoffer, A., Schnaiter, M., an Andreae, M. O.: Spectral light absorption by ambient aerosols influenced by biomass burning in the Amazon Basin. I: comparison and field calibration of absorption measurement techniques, Atmos. Chem. Phys., 6, 3443-3462, doi:10.5194/acp-6-3443-2006, 2006.

Seibert, P., Beyrich, F., Gryning, S. E., Joffre, S., Rasmussen, A., and Tercier, P.: Review and intercomparison of operational methods for the determination of the mixing height, Atmos. Environ., 34. 1001-1027, doi:10.1016/S1352-2310(99)00349-0, 2000.

Virkkula, A., Mäkelä, T., Hillamo, R., Yli-Tuomi, T., Hirsikko, A., Hämeri, K., and Koponen, I. K.: A simple procedure for correcting loading effects of aethalometer data, J. Air & Waste Manage. Assoc., 57, 1214-1222, doi:10.3155/1047-3289.57.10.1214 , 2007.

Vogelezang, D. H. P., and Holtslag, A. A. M.: Evolution and model impacts of alternative boundary layer formulations, Boundary-Layer Meteorol., 81, 245-269, doi:10.1007/BF02430331, 1996.

Weingartner, E., Saathoff, H., Schnaiter, M., Streit, N., Bitnar, B., and Baltensperger, U.: Absorption of light by soot particles: determination of the absorption coefficient by means of aethalometers, J. Aerosol Sci., 34, 1445-1463, doi:10.1016/S0021-8502(03)00359-8, 2003.

Zhang, D. Z., Chen, B., Yamada, M., Niu, H. Y., Wang, B., Iwasaka, Y., and Shi, G. Y.: Elevated soot layer in polluted urban atmosphere: a case study in Beijing, J. Meteorol. Soc. Japan, 90, 361-375, doi:10.2151/jmsj.2012-302, 2012.